Polarized Absorption Spectra of Single-Walled 4 Å Carbon Nanotubes Aligned in Channels of an $AlPO_4$-5 Single Crystal

Z. M. Li,[1] Z. K. Tang,[1,*] H. J. Liu,[1] N. Wang,[1] C. T. Chan,[1] R. Saito,[2] S. Okada,[3] G. D. Li,[4] J. S. Chen,[4] N. Nagasawa,[5] and S. Tsuda[5]

[1]*Department of Physics and Institute of Nano Science and Technology, Hong Kong University of Science & Technology, Clear Water Bay, Kowloon, Hong Kong, China*

[2]*Department of Electronic Engineering, University of Electro-Communications, 1-5-1 Chofugaoka, Chofu-shi, Tokyo 182-8585, Japan*

[3]*Institute of Physics, University of Tsukuba, 111, Tennodai, Tsukuba 305-8577, Japan*

[4]*Key Laboratory of Inorganic Synthesis and Preparative Chemistry, Department of Chemistry, Jilin University, Changchun 130023, China*

[5]*Department of Physics, University of Tokyo, Hongo, Bunkyo-ku, Tokyo 113-0033, Japan*

(Received 23 April 2001; published 29 August 2001)

We report the polarized optical absorption spectra of single-walled 4 Å carbon nanotubes arrayed in the channels of an $AlPO_4$-5 single crystal. When the light electric field (E) is polarized parallel to the tube direction (c), the spectra display a sharp peak at 1.37 eV, with two broadbands at 2.1 and 3.1 eV. In the $E \perp c$ configuration, the tube is nearly transparent in the measured energy region 0.5–4.1 eV. The optical dipole selection rules are discussed, and the absorption bands are assigned to the dipole transitions between the Van Hove singularities. The measured absorption spectra agreed well with the *ab initio* calculations of band structure based on the local density function approximation.

DOI: 10.1103/PhysRevLett.87.127401 PACS numbers: 78.67.Ch, 61.46.+w, 73.22.-f, 82.75.Mj

In 1993, Iijima's group as well as Bethune's group found that the use of transition-metal catalysts leads to nanotubes with only a single wall [1]. A single-walled carbon nanotube (SWNT) is wrapped from a two-dimensional graphite sheet. The diameter of each freestanding SWNT ranges from 0.7 to a few tens of nanometers with a maximum length of about 1 μm. Within the band-folding scheme, the diameter and the chirality of a SWNT are believed to determine whether the nanotube is metallic or semiconducting [2]. Their electronic densities of states have Van Hove singularities, which have been directly observed by scanning tunneling spectroscopy [3]. Optical absorption spectra have been measured for bundles of SWNTs and nanotube thin films [4]. The absorption bands can be attributed to optical transitions between the Van Hove singularities. More controlled experimental studies on the optical properties for SWNTs are, however, not easy to carry out because of the technical difficulty in fabricating *monosized* and *well-aligned* nanotubes. Recently, SWNTs with a diameter as small as 4 Å have been produced in the 1 nm-sized channels of the $AlPO_4$-5 single crystals (AFI in the zeolite terminology) [5,6]. Very recently, one-dimensional superconducting fluctuation with a mean-field superconducting temperature of 15 K has been observed in the 4 Å SWNTs [7]. A 4 Å nanotube has also been synthesized by the mass-selected carbon ion beam deposition as the inner shell of an eighteen-layered multiwalled nanotube [8]. The system of the monosized SWNTs stabilized in the zeolite channels brings the experimental results much closer to the reality of theoretical predictability.

In this Letter, we report polarized absorption spectra for the 4 Å SWNTs arrayed in the one-dimensional channels of an AFI single crystal. AFI is a type of porous aluminophosphate single crystal. Its framework consists of alternate tetrahedra of $(AlO_4)^-$ and $(PO_4)^+$ which form open one-dimensional channels packed in the hexagonal structure. Figure 1a schematically shows the framework structure of the AFI single crystal viewed along the [001] direction. The typical dimension of the AFI crystals used in our experiment is about 100 μm in diameter and about 300 μm in length. The AFI single crystals are transparent from the near infrared to the ultraviolet region; they are therefore ideal hosts to study optical properties of nanostructures formed inside. A detailed fabrication process of our samples was reported elsewhere [5,6]. The AFI single crystal containing nanotubes behaves as a good polarizer with high absorption for light polarized parallel to

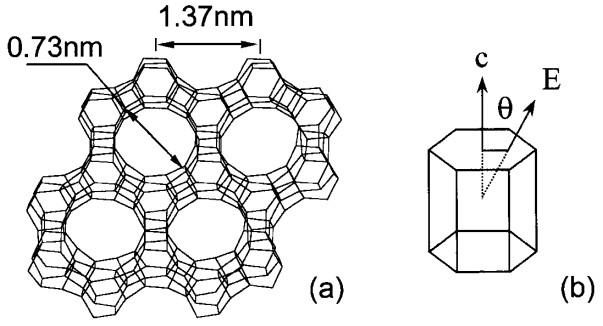

FIG. 1. (a) The framework structure of an AFI single crystal viewed along the [001] direction. (b) A schematic show of the AFI single crystal and light polarization configuration.

the channel direction ($E \parallel c$) and high transparency for the $E \perp c$ polarization.

In order to easily handle the small crystal, the SWNT-containing AFI crystal was horizontally fixed inside a hole (500 μm diameter) drilled on a machinable ceramic plate using epoxy resin. After the resin became hardened, the sample was polished mechanically then using Ar-ion milling to as thin as 10 μm. Transmission spectra were measured at room temperature, using a tungsten-halogen incandescent lamp as a light source. The incident polarized light was focused onto the sample by a reflecting microscope objective. The transmission light was collected by another reflecting objective coupled with an optical fiber and dispersed by a 275-nm single-grating monochromator.

Figure 2 is a high-resolution transmission electron microscope (HRTEM) image (JEOL2010 electron microscope, operating at 200 kV) of our nanotubes. The AFI framework was removed using hydrochloric acid before the TEM observation [9]. We can see many parallel doubled dark lines, which are typical images of SWNTs. The diameter of the SWNTs is determined to be 0.42 ± 0.02 nm. Because of the small diameter, there are only three limited possible chiralities, the zigzag $(5, 0)$, the armchair $(3, 3)$, and the chiral $(4, 2)$ tubules whose diameters are, respectively, 0.40, 0.41, and 0.42 nm. The system energies of these nanotubes are similar to each other, with only a slight difference in the order $E_{(4,2)} \leq E_{(3,3)} \leq E_{(5,0)}$ for the freestanding tubes. However, the abundance of these tubes is not necessarily governed by this order since the steric constraint of the limited channel space may favor the smaller $(5, 0)$ tube; in addition, the kinetics of the formation process would be an important factor to consider.

Figure 3 shows a series of optical absorption spectra (plotted in optical density, OD) of the SWNT-containing AFI crystal for different polarization configurations. The top curve labeled 0° corresponds to the absorption of light polarized parallel to the tube axis ($E \parallel c$; see Fig. 1b). In this spectrum, we see a sharp peak at 1.37 eV with a shoulder at 1.19 eV, and two broadbands centered at 2.1 and 3.1 eV, respectively. The intensities of these absorption bands gradually decrease with increasing polarization angle (the increment is 10°). For the perpendicular configuration ($E \perp c$), the absorption bands vanish eventually and the nanotube is nearly transparent in the whole measured energy region, as indicated by the rather flat curve labeled 90°. As a reference, the absorption spectrum of the pristine zeolite is shown in the bottom of Fig. 3. We could not carry out the measurement in the energy region higher than 4.0 eV, because the epoxy used to hold the sample has strong absorption in the ultraviolet region. The inset of Fig. 3 shows the normalized absorbance $\mathcal{A}$ [$\equiv 1 - T = 1 - \exp(-OD)$, where T is the transmittance] of the absorption bands, plotted as a function of polarization angle θ. The squares, open circles, and solid circles are for the absorption bands A, B, and C, respectively. As seen in the inset, all of them can be well

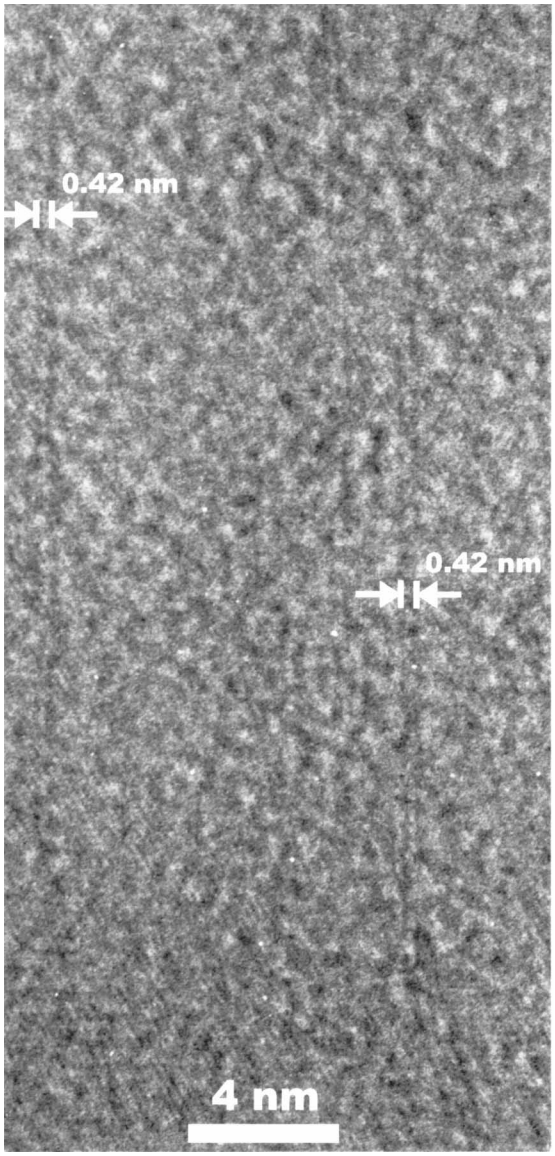

FIG. 2. HRTEM image of the SWNTs. The nanotubes were moved out from the AFI channels and dispersed on a carbon lacey film for the TEM observation.

fitted by using a $\cos^2\theta$ line shape (solid curve) [10]. It is worth indicating that small-width graphite ribbons could also exhibit Van Hove singularities that are qualitatively similar to those observed for SWNTs [11,12]. However, the absorption in Fig. 3 cannot be explained by graphite ribbons because of the following reasons. First, small graphite ribbons are very unstable, as there are too many dangling bonds at the edge sites. These dangling bonds should be terminated by other atoms, for instance, hydrogen atoms. Second, the zeolite channel is too small to hold hydrogen-terminated graphite ribbons except maybe those ultranarrow ones with two or at most three carbon atoms in width, and the local density approximation (LDA) calculated energy gap [12] between the occupied and unoccupied Van Hove singularities for narrow ribbons is much higher than the lowest dipole transition energy (A band in Fig. 3).

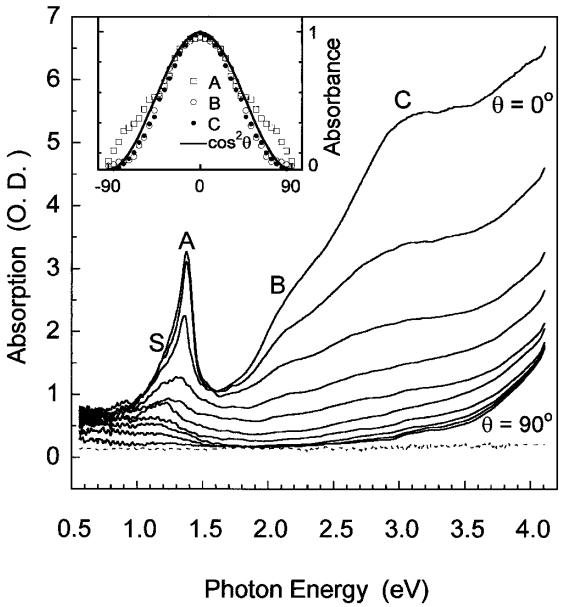

FIG. 3. The polarized optical absorption spectra of the SWNT-containing AFI crystal. The curves labeled by $\theta = 0°$ and $\theta = 90°$ are for the $E \parallel c$ and the $E \perp c$ polarization configurations, respectively. The dotted curve (bottom) is the spectrum of the AFI crystal.

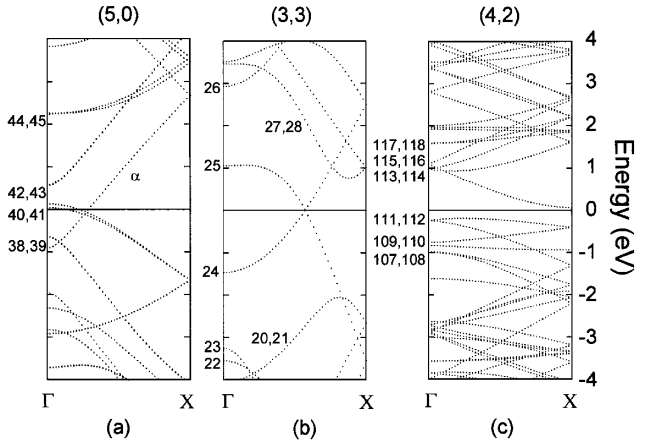

FIG. 4. Calculated energy band structures for (a) zigzag $(5,0)$, (b) armchair $(3,3)$, and (c) chiral $(4,2)$ nanotubes; the Fermi level is at 0. The number shown in the figure is the order of the energy levels counted from the bottom.

It is noticed that in the $E \parallel c$ configuration, the nanotubes have a finite optical density within the whole photon energy region, which implies that these ultrasmall nanotubes are of metallic behavior (π-electron plasma absorption background [13]). The metallic behavior along the tube direction was also seen from the electric transport measurements [14]. Based on the band-folding scheme, tube $(5,0)$ should be semiconducting. However it is not the case for such a small nanotube, where large curvature effects would lead to a hybridization of σ^* and π^* orbitals [15], so the electronic structures can no longer be predicted by the simple band-folding picture. To understand the electronic properties of such small nanotubes, we performed *ab initio* calculations for these three nanotubes, using a plane-wave pseudopotential formulation [16] within the framework of LDA [17]. We use a supercell geometry [15] so that the tubes are aligned in a hexagonal array with the closest distance between adjacent tubes being 6 Å, which permits negligible tube-tube interactions. The calculated energy band structures are shown in Fig. 4. The curvature effects lowered the antibonding π band (marked by α) to cross the Fermi energy, leading to the $(5,0)$ nanotube being metallic as shown in Fig. 4a. The $(3,3)$ nanotube is metallic, as expected, while the $(4,2)$ nanotube has a small indirect energy gap at the Fermi energy (see Figs. 4b and 4c). The optical dipole transition has selection rules for polarizations parallel or perpendicular to the nanotube axis. As we show the polarization dependence of the spectra, there is no absorption for the light polarized perpendicular to the nanotube axis, which could be ascribed to the depolarization effect [18]. Since the present sample is well aligned and well separated to each other, the depolarization effect appears almost perfectly. Hereafter we consider only the polarization parallel to the nanotube axis. The optical absorptions result from the dipole transitions from the bonding π bands to the antibonding π bands. Although there are many possible pairs for bonding and antibonding π bands, the dipole allowed pairs of energy subbands are limited to only a few. Thus we can assign the chiralities and the energy subbands to the observed absorption spectra. The symmetries of tubes $(5,0)$, $(3,3)$, and $(4,2)$ correspond to the D_{5d}, D_{3d}, C_{28} groups, respectively. Further analysis of selection rules for $E \parallel c$ polarization shows that the allowed dipole transitions are $A_{1g} \rightarrow A_{2u}$, $A_{2g} \rightarrow A_{1u}$, $E_{1g} \rightarrow E_{1u}$, and $E_{2g} \rightarrow E_{2u}$ for D_{5d} symmetry; $A_{1g} \rightarrow A_{2u}$, $A_{2g} \rightarrow A_{1u}$, and $E_g \rightarrow E_u$ for D_{3d} symmetry; $A_g \rightarrow A_u$, $B_g \rightarrow B_u$, and $E_{jg} \rightarrow E_{ju}$, $j = 1, 2, \ldots, 13$ for C_{28} symmetry, respectively. The symmetry assignments for the calculated energy subbands were taken by looking at the real part of the wave function from which we can see not only the symmetry but also the character of the wave functions such as the σ or π orbitals. The sharp absorption peak A at 1.37 eV (Fig. 3) is assigned to the calculated $E_{1g} \rightarrow E_{1u}$ transition (1.20 eV) of the (5,0) zigzag tubes and the $E_{9g} \rightarrow E_{9u}$ transition (1.21 eV) to the (4,2) chiral tubes. It is noted that there is a shoulder S at the low energy side of the A band. This shoulder is attributed to the dipole $E_{10g} \rightarrow E_{10u}$ transition (1.00 eV) at the X point of the (4,2) chiral tubes. For the energy region higher than 2.0 eV, several transitions may be assigned: for example, the $E_{10g} \rightarrow E_{10u}$ transition (1.89 eV) of the (4,2) chiral tubes near the band B; $E_g \rightarrow E_u$ transition (2.81 eV) of the (3,3) tube and $E_{3g} \rightarrow E_{3u}$ transition (2.57 eV) of the (4,2) tube near the band C. Since the energy dispersion is relatively large, we expect broad absorption spectra. All possible dipole allowed transitions of the three type of nanotubes in the measured photon energy region are summarized in Table I. It is

TABLE I. Allowed dipole transitions of tubes (5,0), (3,3), and (4,2) corresponding to the absorption bands S, A, B, and C.

	(5, 0)	(3, 3)	(4, 2)
S (1.2 eV)			$109(E_{10g}) \rightarrow 115(E_{10u})$
A (1.37 eV)	$38\&39(E_{1g}) \rightarrow 42\&43(E_{1u})$		$111\&112(E_{9g}) \rightarrow 113\&114(E_{9u})$
B (2.1 eV)			$109\&110(E_{10g}) \rightarrow 115\&116(E_{10u})$
C (3.1 eV)		$20\&21(E_g) \rightarrow 27\&28(E_u)$	$107\&108(E_{3g}) \rightarrow 117\&118(E_{3u})$

known that the energy gap is usually underestimated in the LDA calculations. Thus, if a constant value of about 0.17 eV is added to all of the above transition energies, the calculation results are in good agreement with the measured absorption spectra [19].

In summary, we report the anisotropic optical absorption for the 4 Å nanotubes confined in zeolite channels. The advantages of the ultrasmall nanotubes are (1) single-wall nanotubes are separated from one another in channels of zeolite crystal, (2) the diameter and chirality of nanotube (n, m) are very limited, and (3) the alignment of the nanotube is almost perfect in the single crystal of zeolite. Thus the depolarization effect predicted by theory [18] and observed in isolated nanotube Raman spectroscopy is clearly observed in well-aligned and single-walled nanotubes. Since the zone-folding tight-binding calculation is not suitable for such small nanotubes, we calculated the electronic states of single-wall nanotubes with chirality (5,0), (3,3), and (4,2), which are only possibilities, by *ab initio* pseudopotential calculations. With the help of the group theory, we got a unique assignment of the possible dipole transitions to the observed spectra. The combination of theory and experiment was thus in a very good manner to explain this exotic material.

We are grateful to Professor P. Sheng for stimulating discussions, and to Dr. W. K. Ge for his comments. This research was supported by the RGC Grants No. HKUST 6152/99P and No. 6128/98P. R. S. acknowledges a Grant-in-Aid (No. 13440091) from the Ministry of Education. G. D. L. and J. S. C. acknowledge the support from NSFC.

*Corresponding author.
Email address: phzktang@ust.hk

[1] S. Iijima and T. Ichibashi, Nature (London) **363**, 603 (1993); D. S. Bethune, C. H. Kiang, M. S. de Vries, G. Gorman, R. Savoy, J. Vazquez, and R. Beyens, Nature (London) **363**, 605 (1993).

[2] R. Saito, G. Dresselhaus, and M. S. Dresselhaus, *Physical Properties of Carbon Nanotubes* (Imperial College Press, London, 1998), and related papers therein.

[3] J. W. G. Wildoer, L. C. Venema, A. G. Rinzler, R. E. Smalley, and C. Dekker, Nature (London) **391**, 59 (1998).

[4] H. Kataura, Y. Kumazawa, Y. Maniwa, I. Umezu, S. Suzuki, Y. Ohtsuka, and Y. Achiba, Synth. Met. **103**, 2555 (1999); M. Ichida, S. Mizuno, Y. Tani, Y. Saito, and A. Nakamura, J. Phys. Soc. Jpn. **68**, 3131 (1999).

[5] N. Wang, Z. K. Tang, G. D. Li, and J. S. Chen, Nature (London) **408**, 50 (2000).

[6] Z. K. Tang, H. D. Sun, J. Wang, J. Chen, and G. Li, Appl. Phys. Lett. **73**, 2287 (1998).

[7] Z. K. Tang, L. Y. Zhang, N. Wang, X. X. Zhang, G. H. Wen, G. D. Li, J. N. Wang, C. T. Chan, and P. Sheng, Science **292**, 2462 (2001).

[8] L. C. Qin, X. L. Zhao, K. Hirahara, Y. Miyamoto, Y. Ando, and S. Iijima, Nature (London) **408**, 50 (2000).

[9] N. Wang, G. D. Li, and Z. K. Tang, Chem. Phys. Lett. **339**, 47 (2001).

[10] The projection of the electric field E of light with polarization angle θ is $E\cos\theta$. If only the light polarized along the tube direction could be absorbed by the nanotube, then the absorbance of the light with polarization angle θ will be proportional to $|E\cos\theta|^2 \propto \cos^2\theta$.

[11] K. Nakada, M. Fujita, G. Dresselhaus, and M. S. Dresselhaus, Phys. Rev. B **54**, 17 954 (1996).

[12] Y. Miyamoto, K. Nakada, and M. Fujita, Phys. Rev. B **59**, 9858 (1999).

[13] S. Kazaoui, N. Minami, H. Yamawaki, K. Aoki, H. Kataura, and Y. Achiba, Phys. Rev. B **62**, 1643 (2000).

[14] Z. K. Tang, H. D. Sun, and J. N. Wang, Physica (Amsterdam) **279B**, 200 (2000).

[15] X. Blase, Lorin X. Benedict, Eric L. Shirley, and Steven G. Louie, Phys. Rev. Lett. **72**, 1878 (1994).

[16] G. Kresse and J. Hafner, Phys. Rev. B **47**, 558 (1993); **55**, 11 169 (1996); G. Kresse and J. Furthmuller, Comput. Mater. Sci. **6**, 15 (1996).

[17] P. Hohenberg and W. Kohn, Phys. Rev. **136**, B864 (1964); W. Kohen and L. J. Sham, Phys. Rev. **140**, A1133 (1965).

[18] H. Ajiki and T. Ando, Physica (Amsterdam) **201B**, 349 (1994).

[19] We note that the graphite bands are stretched by about 14% due to self-energy corrections. When this is taken into account, the calculated transition energies are in very good agreement with experimentally observed values. See S. G. Louie, in *First-Principles Theory of Electron Excitation Energies in Solids, Surfaces, and Defects,* edited by C. Y. Fong, Topics in Computational Materials Science (World Scientific, Singapore, 1997), p. 96.